Title

Heparan Sulfate Modulates Neutrophil and Endothelial Function in Antibacterial Innate Immunity

Journal

Infection and Immunity, 83(9)

ISSN

0019-9567

Authors

Xu, Ding
Olson, Joshua
Cole, Jason N
et al.

Publication Date

2015-09-01

DOI

10.1128/iai.00545-15

Peer reviewed

IAI Journals.ASM.org

Heparan Sulfate Modulates Neutrophil and Endothelial Function in Antibacterial Innate Immunity

Ding Xu,[a,c,f] Joshua Olson,[b] Jason N. Cole,[a,b,g] Xander M. van Wijk,[a,c] Volker Brinkmann,[h] Arturo Zychlinsky,[h] Victor Nizet,[a,b,d] Jeffrey D. Esko,[a,c] Yung-Chi Chang[a,b,e]

Glycobiology Research and Training Center,[a] Department of Pediatrics,[b] Department of Cellular and Molecular Medicine,[c] and Skaggs School of Pharmacy and Pharmaceutical Sciences,[d] University of California, San Diego, La Jolla, California, USA; Graduate Institute of Microbiology, College of Medicine, National Taiwan University, Taipei, Taiwan[e]; Department of Oral Biology, University at Buffalo, School of Dental Medicine, The State University of New York, Buffalo, New York, USA[f]; School of Chemistry and Molecular Biosciences and Australian Infectious Diseases Research Centre, The University of Queensland, St. Lucia, Queensland, Australia[g]; Department of Cellular Microbiology, Max Planck Institute for Infection Biology, Berlin, Germany[h]

Recently, we showed that endothelial heparan sulfate facilitates entry of a bacterial pathogen into the central nervous system. Here, we show that normal bactericidal activity of neutrophils is influenced by the sulfation pattern of heparan sulfate. Inactivation of heparan sulfate uronyl 2-*O*-sulfotransferase (Hs2st) in neutrophils substantially reduced their bactericidal activity, and Hs2st deficiency rendered mice more susceptible to systemic infection with the pathogenic bacterium group B *Streptococcus*. Specifically, altered sulfation of heparan sulfate in mutant neutrophils affected formation of neutrophil extracellular traps while not influencing phagocytosis, production of reactive oxygen species, or secretion of granular proteases. Heparan sulfate proteoglycan(s) is present in neutrophil extracellular traps, modulates histone affinity, and modulates their microbial activity. Hs2st-deficient brain endothelial cells show enhanced binding to group B *Streptococcus* and are more susceptible to apoptosis, likely contributing to the observed increase in dissemination of group B *Streptococcus* into the brain of Hs2st-deficient mice following intravenous challenge. Taken together, our data provide strong evidence that heparan sulfate from both neutrophils and the endothelium plays important roles in modulating innate immunity.

Heparan sulfate (HS) proteoglycans (HSPGs) are ubiquitously expressed by animal cells and play essential roles in cell signaling and cell-cell interactions (1, 2). To a large extent, these properties depend on the interaction of HS with various signaling receptors and their ligands (3). Many pathogens have evolved to exploit cell surface HS molecules as counterreceptors for adhesion and invasion (4–7). Cell surface HSPGs also modulate the innate immune response by regulating chemokine presentation and growth factor responses (8). Thus, HSPGs lie at a nexus between pathogen invasion and host defense.

Neutrophils, the most abundant circulating leukocyte, represent a critical first line of mammalian host defense against a wide range of infectious pathogens. Neutrophils are recruited to sites of infection, recognize and phagocytose microbes, and kill pathogens through a combination of microbicidal mechanisms, including production of reactive oxygen species, release of antimicrobial peptides, and expulsion of their nuclear contents to form neutrophil extracellular traps (NETs) (9, 10). HS modulates the rapid recruitment of neutrophils to sites of infection or injury at different levels, in particular through its interactions with cytokines, chemokines, and selectins (8). We reported previously that reduced expression and altered sulfation of HS on endothelial cells, achieved by inactivating glucosamine *N*-deacetylase-*N*-sulfotransferase-1 (Ndst1) or uronyl 2-*O*-sulfotransferase (Hs2st), altered neutrophil extravasation to sites of sterile inflammation by modifying interactions between endothelial HS and L-selectins on neutrophils and chemokines released during the inflammatory response (11, 12). In contrast, the same modifications of HS on the neutrophil cell surface did not affect trafficking during sterile inflammation (11, 12) and had only mild effects on the acquired immune responses (13). Here we extended this line of investigation to live-bacterial-infection models to probe how HS modification can influence intrinsic neutrophil functions relevant to antibacterial defense and microbicidal activity.

Several potential neutrophil bactericidal effectors, including proteases (elastase and cathepsin G) and α-defensins, have been shown to interact with HSPGs and affect their intracellular localization and retention within granules (14–16). During NET formation at tissue foci of infection, antimicrobial effectors, including elastase, cathepsin G, and strongly cationic histones, are displayed across the chromatin-based network to act against bacteria ensnared in the extracellular structures (17, 18). The polyanionic charge of HS should favor interaction with positively charged histones with the potential to modulate their cytotoxic effects (19–22). Thus, we sought to understand whether modification of HS sulfation in neutrophils could regulate their antimicrobial activity, especially in the context of NETs during *in vivo* infection.

Received 27 April 2015 **Returned for modification** 20 May 2015
Accepted 26 June 2015

Accepted manuscript posted online 6 July 2015

Citation Xu D, Olson J, Cole JN, van Wijk XM, Brinkmann V, Zychlinsky A, Nizet V, Esko JD, Chang Y-C. 2015. Heparan sulfate modulates neutrophil and endothelial function in antibacterial innate immunity. Infect Immun 83:3648–3656. doi:10.1128/IAI.00545-15.

Editor: B. A. McCormick

Address correspondence to Jeffrey D. Esko, jesko@ucsd.edu, or Yung-Chi Chang, yungchiychang@ntu.edu.tw.

Supplemental material for this article may be found at http://dx.doi.org/10.1128/IAI.00545-15.

doi:10.1128/IAI.00545-15

Here we took advantage of conditional knockout mice in which Hs2st is deleted in myeloid cells (including neutrophils) and endothelial cells by excision of a *loxP*-flanked allele under the control of Cre recombinase driven by the Tie2 promoter (*Hs2st*$^{f/f}$ *Tie2 Cre*$^{+}$ mice, referred to here as Hs2st-deficient or mutant mice). Analysis of these animals revealed that neutrophil-derived HS plays a significant role in controlling bactericidal activity. Whereas inactivation of Hs2st on endothelial cells facilitates neutrophil infiltration to sterile inflammatory stimuli (11), the impaired intrinsic bactericidal activity of Hs2st-deficient neutrophils results in increased susceptibility of Hs2st-deficient mice to invasive bacterial infection. The bactericidal defect in Hs2st-deficient mice correlates with reduced NET formation and altered histone affinity to HS within the NETs.

MATERIALS AND METHODS

Bacteria and mouse strains. Human serotype V group B *Streptococcus* (GBS) clinical isolate NCTC 10/84 (ATCC 49447) was propagated in Todd-Hewitt broth (THB; Difco, BD Diagnostics) at 37°C without shaking. For infection studies, bacteria were grown at to mid-exponential phase, resuspended to an optical density at 600 nm (OD_{600}) of 0.4 (~2×10^8 CFU per ml), and serially diluted to the desired inoculum. *Hs2st*$^{f/f}$ *Tie2 Cre*$^{+}$ mice were generated as described previously (11) and backcrossed >10 generations on a C57BL/6 background. Littermate *Hs2st*$^{f/f}$ *Tie2 Cre*$^{-}$ mice were used as wild-type controls in all experiments. Mice were provided *ad libitum* with Nanopure water and PicoLab 5053 lab chow.

Macrophage, neutrophil, and endothelial cell isolation and culture. Murine bone marrow-derived macrophages (MBDMs) were derived from cells collected from femur and tibia marrow and cultured with the conditioned medium collected from L929 cells stably expressing macrophage colony-stimulating factors for 7 days. For neutrophil isolation from murine bone marrow, cells were resuspended in ammonium-chloride-potassium (ACK) lysis buffer to eliminate erythrocytes, resuspended in 45% Percoll (GE Healthcare Life Sciences), layered on discontinuous Percoll gradient solutions (50%, 55%, 62%, and 81%), and centrifuged for 30 min at 1,200 × *g* without a centrifugal brake. Neutrophils were collected from the 62%-81% interface, washed twice with phosphate-buffered saline (PBS), and resuspended in RPMI 1640 containing 2% fetal bovine serum (FBS) for experiments. Neutrophil purity was consistently 85 to 95% as determined by flow cytometry performed with fluorescein isothiocyanate (FITC)-conjugated anti-Gr-1 monoclonal antibody (MAb) (clone RB6-8C5; Caltag Medsystems). For lipopolysaccharide (LPS)-elicited peripheral neutrophils, dorsal air pouches were created by subcutaneous injection of mice with 2.5 ml of sterile air twice every 3 days over a 1-week period. LPS (2 μg) in 0.6 ml 0.5% carboxymethyl cellulose solution (sodium salt; Sigma) was injected into the pouch to recruit neutrophils. Four hours after LPS injection, pouches were lavaged with PBS containing 3 mM EDTA to extract neutrophils; purity was ~90% by flow cytometry. Murine brain microvascular endothelial cells (BMECs) were isolated from the cerebral cortex as described previously (23), except that cells were selected with 5 μg/ml puromycin for 4 days in low-glucose Dulbecco's modified Eagle medium (DMEM) containing 20% FBS, 50 μg/ml endothelial cell growth supplement (Biomedical Technologies, Inc.), 50 μg/ml heparin (Sigma), nonessential amino acids, penicillin, and streptomycin. Cell purity was >98% as assessed by blood endothelial markers (CD31, CD34, CD105, and CD166).

Murine whole blood bactericidal assay. Whole blood was collected by cardiac puncture from euthanized mice with lepirudin to prevent coagulation and to avoid potential confounding effects of heparin in the assay. Blood (300 μl) was mixed with 10^4 CFU of GBS (in 100 μl) and incubated at 37°C in a siliconized microtube under rotation ($n = 2$ or 3 biological replicates). Twenty-five microliters of the mixture was removed at various time points to enumerate CFU of surviving bacteria.

BMDM bactericidal activity and cytokine release. For bacterial killing, 10^5 CFU of the GBS strain NCTC 10/84 were added to 5×10^5 BMDMs (multiplicity of infection [MOI] = 0.2) for 1 h; then 50 μl of 0.6% Triton X-100 was added to lyse cells. The number of CFU of GBS recovered was determined. To detect cytokine secretion after GBS infection, 10^5 macrophages were stimulated for 30 min with GBS (MOI = 1), followed by addition of penicillin (5 μg/ml) and gentamicin (10 μg/ml) to prevent bacterial overgrowth. Culture supernatants were collected 24 h after infection, and secretion of tumor necrosis factor alpha (TNF-α) and interleukin 6 (IL-6) was analyzed by enzyme-linked immunosorbent assay (ELISA) (BD Biosciences). For quantitative RT-PCR analysis, RNA was isolated from BMDMs using TRIzol (Life Technologies) 30 min after GBS stimulation (MOI = 10) and used as a template for cDNA preparation by iScript (Bio-Rad). Quantitative PCR was performed using iQ SYBR green supermix (Bio-Rad) per standard protocols. Primer combinations were as follows: for IL-1β, 5′-ACTACAGGCTCCGAGATGAAC-3′ plus 5′-CCCAAGGCCACAGGTATTTT-3′; for TNF-α, 5′-AGCCCACGTCGTAGCAAACCACCAA-3′ plus 5′-ACACCCATTCCCTTCACAGAGCAAT-3′; for GAPDH, 5′-AACTTTGGCATTGTGGAAGGGC-3′ plus 5′-GGTAGGAACACGGAAGGCCATG-3′. Primers for IL-10 were obtained from the QuantiTect primer assay (Qiagen).

Neutrophil bactericidal activity and extracellular-trap (NET) formation. For bactericidal assays, murine bone marrow neutrophils were pretreated with 160 μM phorbol myristate acetate (PMA) for 90 min, whereas LPS-elicited neutrophils were used directly upon isolation. GBS (2×10^5 CFU) were added to 10^6 neutrophils (MOI = 0.2) and incubated at 37°C with rotation in a siliconized microtube; CFU were measured in 25-μl aliquots at various time points to enumerate surviving GBS. To quantify NET formation after GBS infection, LPS-elicited neutrophils were resuspended in RPMI 1640 containing 2% FBS at a density of 2×10^6 cells/ml, and 2×10^5 cells (100 μl) were transferred to a well of a 96-well microtiter plate containing 2×10^6 CFU GBS in 100 μl. Plates were centrifuged at 1,600 rpm for 5 min to initiate bacterial-cell contact and subsequently incubated for 2 h. Neutrophils were then washed with PBS, fixed with 4% paraformaldehyde, blocked with 2% BSA–PBS, and stained with anti-H2B rabbit polyclonal antibody (1 μg/ml; GenScript) followed by Alexa Fluor 488-conjugated goat anti-rabbit IgG antibody (Life Technology) to visualize NET formation. Images were acquired using an inverted confocal microscope Olympus FV1000 with Fluoview spectral scanning technology (Olympus). For human NET-mediated bactericidal assays, human neutrophils were isolated from healthy donors by Polymorphprep (Axis-Shield) gradient centrifugation, resuspended to 5×10^6/ml in serum-free RPMI 1640 medium, and stimulated with 25 nM PMA (Sigma) for 3 h to induce NET formation. NETs were then digested with DNase I (10 U/ml; Worthington Biochemical Corp.) or heparan lyase I and III (each 5 mU/ml) at 37°C for 30 min and gently rinsed once with PBS. GBS (5×10^5 CFU) were added to the NETs, centrifuged to initiate contact, and incubated for 30 min at 37°C. Surviving GBS were enumerated by serial plating on Todd-Hewitt broth agar (THA) plates. To visualize heparan sulfate on NETs, human neutrophils were stimulated with 25 nM PMA for 3 h to induce NET formation. Cells were then treated with heparan lyase III (5 mU/ml) at 37°C for 20 min, fixed, and stained with mouse anti-heparan sulfate neoepitope MAb (3G10; US Biological) or rabbit anti-human myeloperoxidase PAb (Dako), followed by Alexa Fluor 488-conjugated goat anti-mouse Abs (Life Technology) or Alexa Fluor 594-conjugated goat anti-rabbit Abs (Life Technology) and DAPI (4′,6′-diamidino-2-phenylindole).

BMEC bacterial binding and apoptosis assays. BMECs were grown to confluence in 24-well plates, infected with 2×10^6 CFU GBS per well, and centrifuged at 1,600 rpm for 5 min to initiate bacterial-cell contact. After 30 min of incubation and extensive washes with PBS, cells were disrupted using 0.025% Triton X-100, and surviving bacterial CFU were quantified by serial dilution plating. To assess GBS-induced apoptosis of BMECs, cells were infected as described above, except that 100 μg/ml of gentamicin and 5 μg/ml of penicillin G were added to prevent bacterial

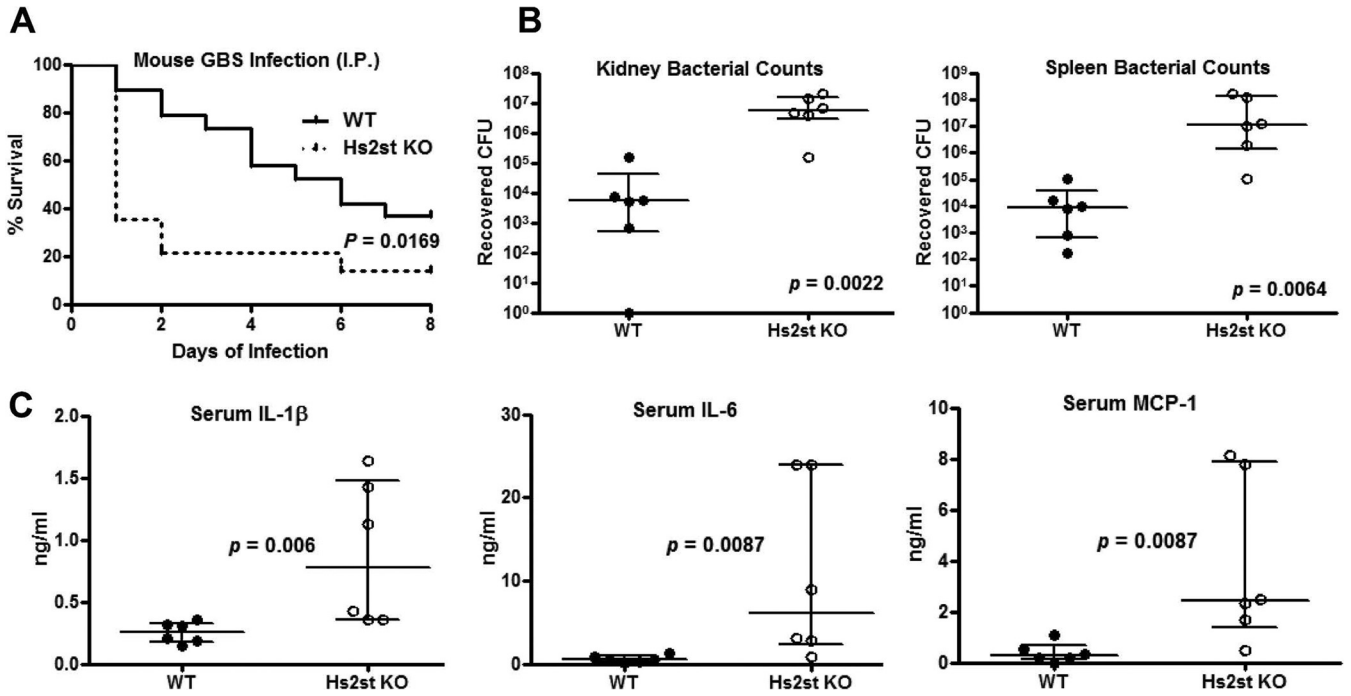

FIG 1 Exacerbated mortality and bacterial dissemination in Hs2St-deficient mice. (A) Increased mortality of Hs2St-deficient mice after GBS challenge. Survival of mice was monitored for 8 days after intraperitoneal (i.p.) infection with 1.5×10^8 CFU GBS. Data were pooled from two independent experiments ($n = 19$ for WT and $n = 14$ for Hs2St-deficient mice). Differences between groups were calculated by a log rank test. Mice were infected i.p. with 5×10^7 CFU of GBS and then euthanized at 18 h postinfection for collection of organs for enumeration of bacterial CFU (B) and inflammatory cytokine ELISA (C). Data are medians with interquartile ranges from one of the two independent experiments. Each circle denotes one mouse ($n = 6$/group). Differences between groups were calculated by Mann-Whitney test (B and C).

overgrowth. Cells were cultured for 4 h or 24 h, and apoptotic cells were stained by TUNEL (terminal deoxynucleotidyltransferase-mediated dUTP-biotin nick end labeling) assay using a kit (BD Biosciences). Data were acquired using BD FACSCalibur and analyzed by CellQuest software.

Western blot analysis. Murine BMDMs were stimulated with GBS (MOI = 5) for 30 min and then lysed in buffer containing 50 mM Tris (pH 8), 150 mM NaCl, 1% NP-40, protease inhibitor cocktail (Roche), and phosphatase inhibitor cocktail (Santa Cruz Biotechnology). Neutrophils were stimulated with 160 nM PMA for 1 h or 2 h before collection of cell lysates and supernatants. Samples were separated on SDS-PAGE and transferred to a polyvinylidene difluoride (PVDF) membrane. The membrane was probed with antibodies recognizing phospho-JNK (Cell Signaling Technology), IκB (Cell Signaling Technology), followed by appropriate horseradish peroxidase (HRP)-conjugated secondary Abs (Bio-Rad) and enhanced chemiluminescence reagent (Thermo Scientific).

Mouse infection studies. All animal experiments were performed using accepted veterinary standards on protocols approved by the UCSD Committee on the Use and Care of Animals. To monitor survival after systemic GBS challenge, mice (10 to 12 weeks old) were infected by intrperitoneal (i.p.) injection with 1.5×10^8 GBS and observed for 8 days. For determination of bacterial organ dissemination and serum cytokine secretion, mice were infected i.p. with 5×10^7 GBS, and spleens, kidneys, and blood were harvested aseptically 18 h postinfection. Serum concentrations of IL-6, IL-1β, and MCP-1 were measured by ELISA (BD Biosciences). In the meningitis model, mice (10 to 12 weeks old) were infected intravenously (i.v.) with 1.4×10^8 GBS, and the number of bacterial CFU in the blood was examined 4 h later to ensure sure similar initial bacterial burdens. Mice were euthanized 18 h after infection, and samples of blood, brain/meninges, lung, spleen, and kidney were collected aseptically. Bacterial CFU in blood and tissue homogenates were determined by serial dilution plating. Bacterial counts in brain were corrected for their weight differences. Brains collected from infected mice were fixed with 4% formalin, paraffin embedded, and sectioned for hematoxylin-and-eosin (H&E) and Gram staining.

Neutrophil phagocytosis assay. Heat-killed GBS were labeled at room temperature for 1 h with pH-sensitive pHrodo red succinimidyl ester (Life Technology) using a 1 mM final dye concentration. Fresh blood (250 μl), treated with lepirudin as an anticoagulant, was incubated with 2.5×10^6 labeled GBS (MOI, ~100) at either 37°C or 4°C for 1 h with rotation. Samples were treated with ACK lysis buffer (Mediatech, Inc.) to remove erythrocytes and fixed with 2% paraformaldehyde. Preparations were then stained using allophycocyanin (APC)-conjugated rat anti-mouse Ly6G (clone 1A8; BD Biosciences) for 10 min and subjected to fluorescence-activated cell sorting (FACS). The final graph was prepared by gating the Ly6G-positive cell population.

Histone binding assay. Monolayers of cultured primary lung endothelial cells derived from wild-type (WT) and *Hs2st*$^{f/f}$ *Tie2 Cre*$^{+}$ mice were detached using Accutase (Millipore) and incubated with human H2B or H3 (5 μg/ml; New England BioLabs) for 1 h in PBS at 4°C. The cells were then incubated at 4°C for 1 h with rabbit anti-H2B IgG (2 μg/ml; GenScript) or rabbit anti-H3 IgG (1:200; Cell Signaling), followed by Alexa Fluor 647-conjugated anti-rabbit IgG. Cells were subjected to flow cytometry, and histone binding was assessed using FlowJo software (Tree Star, Inc.). For neutrophil binding, whole blood from WT and *Hs2st*$^{f/f}$ *Tie2 Cre*$^{+}$ mice was treated with ACK lysis buffer (Mediatech, Inc.) to remove erythrocytes. The cells were then used to perform histone binding as described above for endothelial cells. The cells were also stained with FITC-conjugated Gr-1 antibody (Life Technology), and Gr-1-positive cells were gated as neutrophils.

Scanning electron microscopy. Samples were fixed with glutaraldehyde and contrasted using repeated incubation with osmium tetroxide and tannic acid. After dehydration in an ethanol series, samples were critical-point dried, coated with a layer of carbon/platinum, and analyzed

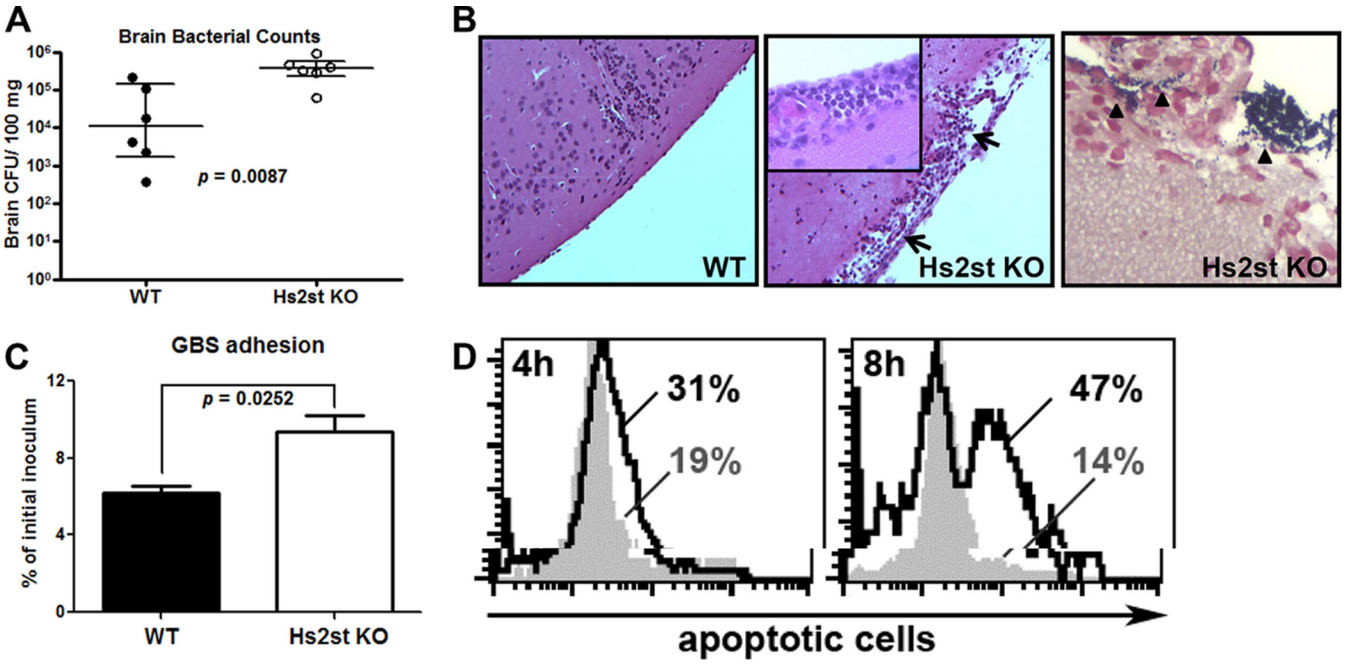

FIG 2 Increased GBS association and apoptosis of the Hs2st-deficient endothelial cells contributed to the GBS brain dissemination. Mice were intravenously challenged with 1.4×10^8 CFU of GBS, and brains were collected 18 h after GBS infection to measure bacterial loads (A) or fixed in formalin for H&E staining (B, left and middle; note the damage to the meninges) and Gram staining (B, right). Data are medians with interquartile ranges from one of the two independent experiments, and each symbol denotes 1 mouse ($n = 6$ for each group). (C) Increased GBS association with Hs2st-deficient mouse brain microvascular endothelial cells (BMECs). Primary isolated BMECs were infected with GBS (MOI = 10) for 30 min, followed by extensive washing to remove unbound GBS. Cell-associated GBS were enumerated by serial plating. Differences between the two groups were calculated by unpaired *t* test. (D) BMECs were infected with GBS at an MOI of 10 for the indicated times, and apoptotic cells were detected by TUNEL assay. Representative data are from one of the 2 or 3 independent experiments (C and D).

at 10 kV in a LEO1550 field emission scanning electron microscope (Zeiss SMT).

Statistical analysis. GraphPad Prism version 5 was used for statistical analysis. Statistical significance was accepted at a *P* value of <0.05. Data shown either were pooled from two independent experiments or are representative data from 2 or 3 independent experiments conducted with biological replicates. The significance of differences between different groups for animal experiments was determined by Mann-Whitney test. Unpaired *t* test was used to compare the difference between different 2 groups.

RESULTS

Hs2st-deficient mice are more susceptible to invasive bacterial infection. Inactivation of Hs2st in endothelial cells (*Hs2st*$^{f/f}$ *Tie2 Cre*) increases neutrophil infiltration during acute sterile inflammation (11), suggesting that Hs2st-deficient mice might resist infection with live bacteria compared to wild-type animals. Surprisingly, when mice were challenged by systemic intraperitoneal infection with the human bacterial pathogen group B *Streptococcus* (GBS), the mutant was dramatically more susceptible to infection (Fig. 1A). Notably, 79% (11 out of 14) of the Hs2st-deficient mice died rapidly within the first 48 h, whereas the wild-type succumbed stepwise over the 8-day monitoring period (Fig. 1A).

To begin to ascertain contributing factors for the higher mortality of Hs2st-deficient mice, animals were challenged with a lower (sublethal) inoculum and the bacterial CFU in multiple organs were measured. GBS dissemination was markedly increased in Hs2st-deficient mice—both kidney and spleen CFU counts were 2 to 3 orders of magnitude greater than those observed in wild-type mice (Fig. 1B). Significantly enhanced serum levels of the proinflammatory cytokines IL-6, IL-1β, and MCP-1 were observed in infected mutant mice (Fig. 1C). These observations indicate that Hs2st-deficient animals were capable of mounting a proinflammatory cytokine response to GBS infection but were less competent in limiting GBS growth or dissemination *in vivo*.

GBS can invade brain microvascular endothelial cells (BMECs) comprising the blood-brain barrier (BBB) to cause meningitis. We showed previously that genetic impairment of HS expression in flies or mice reduced GBS dissemination into the brain (24). To examine how altering 2-*O*-sulfation might influence susceptibility to GBS meningitis, we measured GBS dissemination into brain after intravenous challenge (Fig. 2A). The number of CFU in the brain was increased in the Hs2st-deficient mice compared to wild-type mice at 18 h postinfection. Likewise, Hs2st-deficient mice showed more profound histological evidence of meningeal cell injury as well as increased neutrophil infiltration (Fig. 2B, middle) and GBS dissemination (Fig. 2B, right) into the brain. In tissue culture studies using primary BMECs isolated and prepared from wild-type and Hs2st-deficient animals, we noted that adherence of GBS to the mutant endothelial cells was 50% greater than that to wild-type BMECs (Fig. 2C). Enhanced adhesion of GBS to Hs2st-deficient BMECs correlated with a higher rate of apoptosis (50% at 8 h) than that to wild-type BMECs (14% at 8 h) (Fig. 2D). This finding is consistent with previous studies showing that adherence and invasion of GBS into mammalian cells often provokes apop-

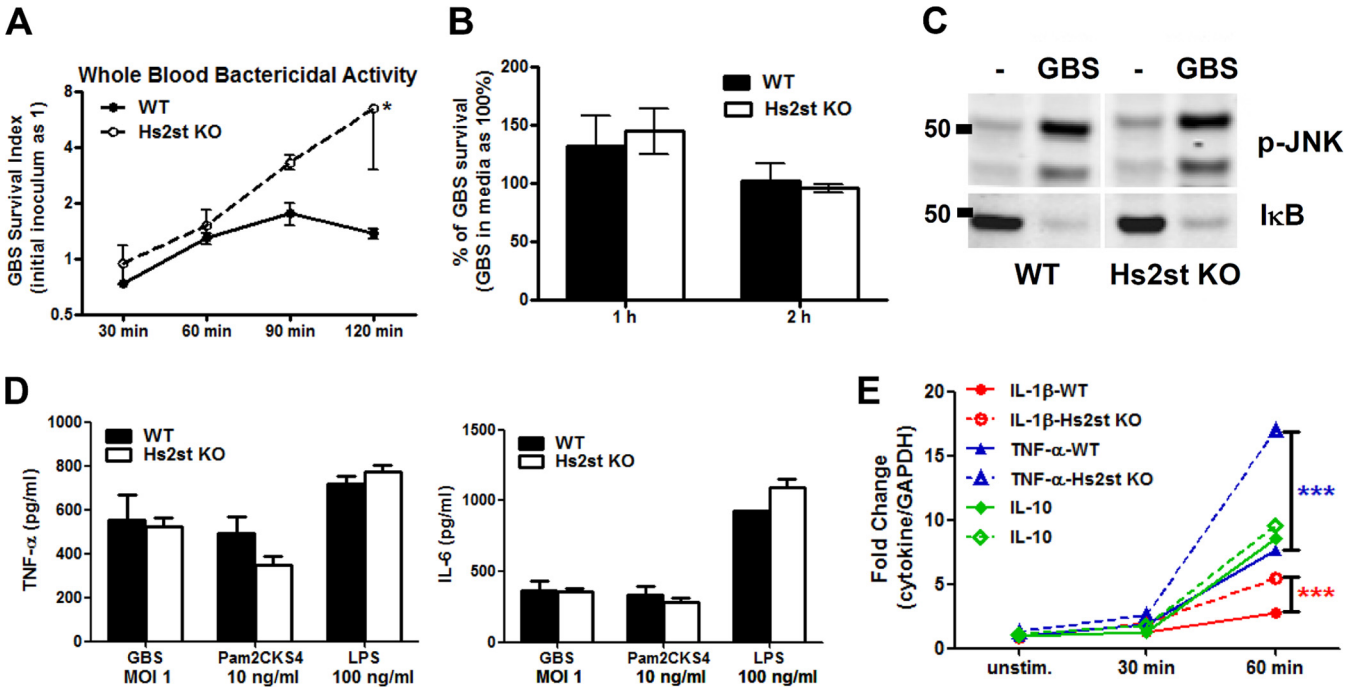

FIG 3 Hs2st-deficient macrophages are competent to respond to bacterial challenge. (A) Increased replication of GBS in whole blood from Hs2St-deficient mice. GBS (10^4 CFU) were incubated with blood collected from WT or Hs2St-deficient mice, and surviving bacteria were enumerated at the indicated time points by serial plating. Data are representative of two independent experiments. (B) Similar bactericidal activity between WT and Hs2st-deficient macrophages. Mouse bone marrow-derived macrophages (MBDMs) were infected with GBS at an MOI of 0.2, and surviving GBS were enumerated at the indicated time point by serial plating. (C) MBDMs from WT and Hs2st-deficient mice were challenged with GBS for 30 min, and cell lysates were collected to analyze IκB degradation and JNK phosphorylation by Western blotting. (D) Macrophage cytokine secretion upon bacterial challenge. MBDMs were challenged with GBS, Pam2CKS4, and LPS for 24 h, and the culture supernatant from the stimulated macrophages was harvested for cytokine ELISA. (E) mRNA was collected from WT and Hs2st-deficient macrophages after GBS stimulation to analyze cytokine transcript production by quantitative RT-PCR. Data are means ± standard errors of the means (SEM) from one of 2 or 3 independent experiments. Differences between groups were calculated by an unpaired *t* test. ***, $P < 0.001$; *, $P < 0.05$ (A, B, D, and E).

tosis (25–28), which may result from more efficient delivery of its cytolytic and proapoptotic β-hemolysin/cytolysin toxin (29).

Wild-type and Hs2st-deficient macrophages respond equally to GBS stimulation. Hs2st deletion driven by the Tie2 promoter targets myeloid cells as well as endothelial cells. To examine whether loss of Hs2st influenced myeloid cell responses to bacterial challenge, we inoculated fresh whole blood from wild-type and Hs2st-deficient mice with GBS and measured bacterial survival over time. Within 2 h, CFU counts in Hs2st-deficient mouse blood increased 6-fold over the initial inoculum, whereas proliferation was controlled in wild-type blood (Fig. 3A). To determine the innate immune cell(s) responsible for this difference in susceptibility, murine bone marrow-derived macrophages were cocultured with GBS. Similar bactericidal capability was observed for wild-type and mutant macrophages (Fig. 3B). As shown in Fig. 3C, c-Jun N-terminal kinase (JNK) phosphorylation and IκB degradation were similar as well, indicating a competent signaling response of the Hs2st-deficient macrophages to GBS infection. Furthermore, secretion of proinflammatory cytokines TNF-α and IL-6 in response to various Toll-like receptor stimuli, such as heat-killed GBS, Pam2CKS4 (synthetic bacterial lipopeptides), and LPS, was comparable in Hs2st-deficient macrophages and in wild-type macrophages (Fig. 3D). At the transcriptional level, mRNA expression for proinflammatory cytokines (TNF-α and IL-1β) and the anti-inflammatory cytokine IL-10 was also similar or greater in Hs2st-deficient macrophages compared to wild-type macrophages (Fig. 3E). All these observations suggest that Hs2st-deficient macrophages are capable of detecting and responding to bacterial challenge.

Hs2st-deficient neutrophils show reduced bactericidal activity and extracellular-trap formation. Neutrophils are the most abundant pathogen-fighting myeloid cells in the circulation and prominent first responders at infectious and inflammatory foci. We hypothesized that dramatically increased GBS dissemination in Hs2st-deficient mice could reflect a defect in Hs2st-deficient neutrophil innate immune function(s). Indeed, Hs2st-deficient bone marrow-derived neutrophils showed a significant defect in bactericidal activity against GBS (Fig. 4A), in contrast to our findings with bone marrow-derived macrophages (Fig. 3B). Diminished bactericidal activity was also observed for Hs2st-deficient neutrophils collected from a dorsal air pouch after LPS-elicited recruitment (Fig. 4B). Our previous study showed that both *Hs2st*$^{f/f}$ *Tie2 Cre*$^{+}$ mice reproduced normally, and no differences in blood leukocyte counts were observed (11). The detail morphology of unstimulated neutrophils was also examined under the electron microscope, and we did not observe difference between WT and Hs2st-deficient neutrophils (see Fig. S1 in the supplemental material). We next analyzed various neutrophil bactericidal functions. Bactericidal activities of neutrophils are multifaceted and include generation of reactive oxygen species (ROS), release of granule proteases and antimicrobial peptides, phagocytosis and killing within the phagolysosome, and formation of neu-

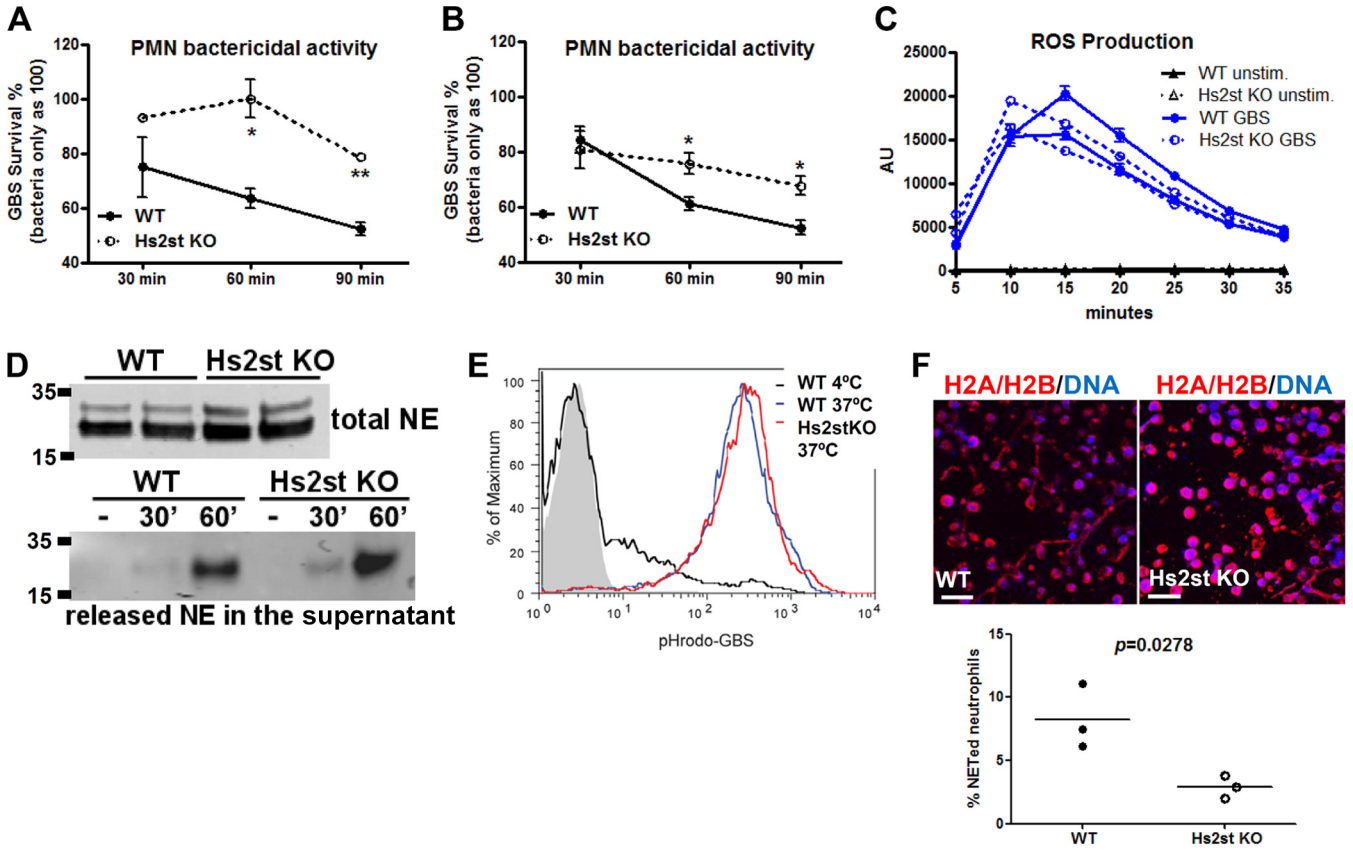

FIG 4 Reduced bactericidal activity of Hs2st-deficient neutrophils. Bone marrow neutrophils (A) and LPS-elicited neutrophils (B) were collected from WT or Hs2St-deficient mice. After challenge with GBS, CFU were measured at the indicated time points by serial plating. Data shown are means ± SEM from one of the two independent experiments. (C) Reactive oxygen species production from bone marrow neutrophils after GBS stimulation detected by a luminol-based assay ($n = 2$ mice). (D) Bone marrow neutrophils were directly lysed or stimulated with GBS for 30 min. Supernatants were collected to measure the total neutrophil elastase (top) or released neutrophil elastase (bottom) by Western blot analysis. (E) Whole blood from WT and Hs2st-deficient mice was incubated with pHrodo red-labeled GBS (MOI of 100) for 1 h at 37°C (phagocytosis) or 4°C (control). Neutrophils were fixed and subjected to flow cytometry to measure internalized GBS. (F) LPS-elicited neutrophils were stimulated with GBS at an MOI of 10 for 2 h, washed, fixed, and stained with H2A/H2B MAb to visualize NET formation. Differences between groups were calculated by an unpaired *t* test. **, $P < 0.01$; *, $P < 0.05$ (A, B, C, and F).

trophil extracellular traps (NETs). We postulated that neutrophils deficient in Hs2st must be crippled in one or more of these antimicrobial mechanisms. Inactivation of Hs2st on the neutrophils did not affect ROS generation (Fig. 4C), synthesis and release of elastase (Fig. 4D), or phagocytic activity by neutrophils (Fig. 4E). However, we observed that Hs2st-deficient neutrophils produced fewer NETs after GBS stimulation, as quantified by immunostaining using antibodies to the H2A/H2B complex and counting the number of neutrophils connected by the NET strands (Fig. 4F).

Alteration of heparan sulfate affects histone binding capacity. Since inactivation of Hs2st on the neutrophils reduced NET formation, we asked if HS is present in NETs and whether alteration of HS sulfation patterns could influence NET structure and function. In subsequent experiments, we analyzed human neutrophils to determine the relevance of our findings in the mouse. Compared to human neutrophils, mouse neutrophils make NETs more slowly and less efficiently. Mouse neutrophils require 16 h to undergo NETosis, and only about 30% of the stimulated cells released NETs during this period. In contrast, it takes only 3 to 4 h for 80% of the human neutrophils to make NETs (30). Freshly isolated human neutrophils were stimulated with PMA to induce NET formation and costained with MAbs specific for HS and myeloperoxidase (MPO). HS is physically present in normal NETs, as revealed by colocalization of HS, MPO, and DNA straining (Fig. 5A). NETs treated with heparan lyase to eliminate HS showed significantly reduced killing of GBS, an effect similar to degrading the extracellular DNA backbone of the NETs with DNase (Fig. 5B). Thus, HS is a component of NETs whose presence is required for NET-mediated bactericidal activity of neutrophils.

Scanning electron microscopy showed that although NETs were diminished in Hs2st-deficient neutrophils, their ultrastructural characteristics were similar to those generated by wild-type neutrophils. However, NETs from Hs2st-deficient neutrophils had more attached globular domains (Fig. 5C), which may reflect histones and other proteins associated with NETs. Consistent with these data, we found that histones H2B and H3 showed greater binding to HS expressed on the surface of Hs2st-deficient neutrophils than wild-type endothelial cells. The relative fluorescence units are 4 and 5 (after subtracting the background fluorescence reading) for H2B binding and 4.1 and 11.6 for H3 binding in wild-type and mutant neutrophils, respectively. This represents a 25% increase of H2B binding and a 180% increase of H3 binding in mutant neutrophils, which suggests that the NETs derived from Hs2st-deficient mice might contain HS with greater binding ca-

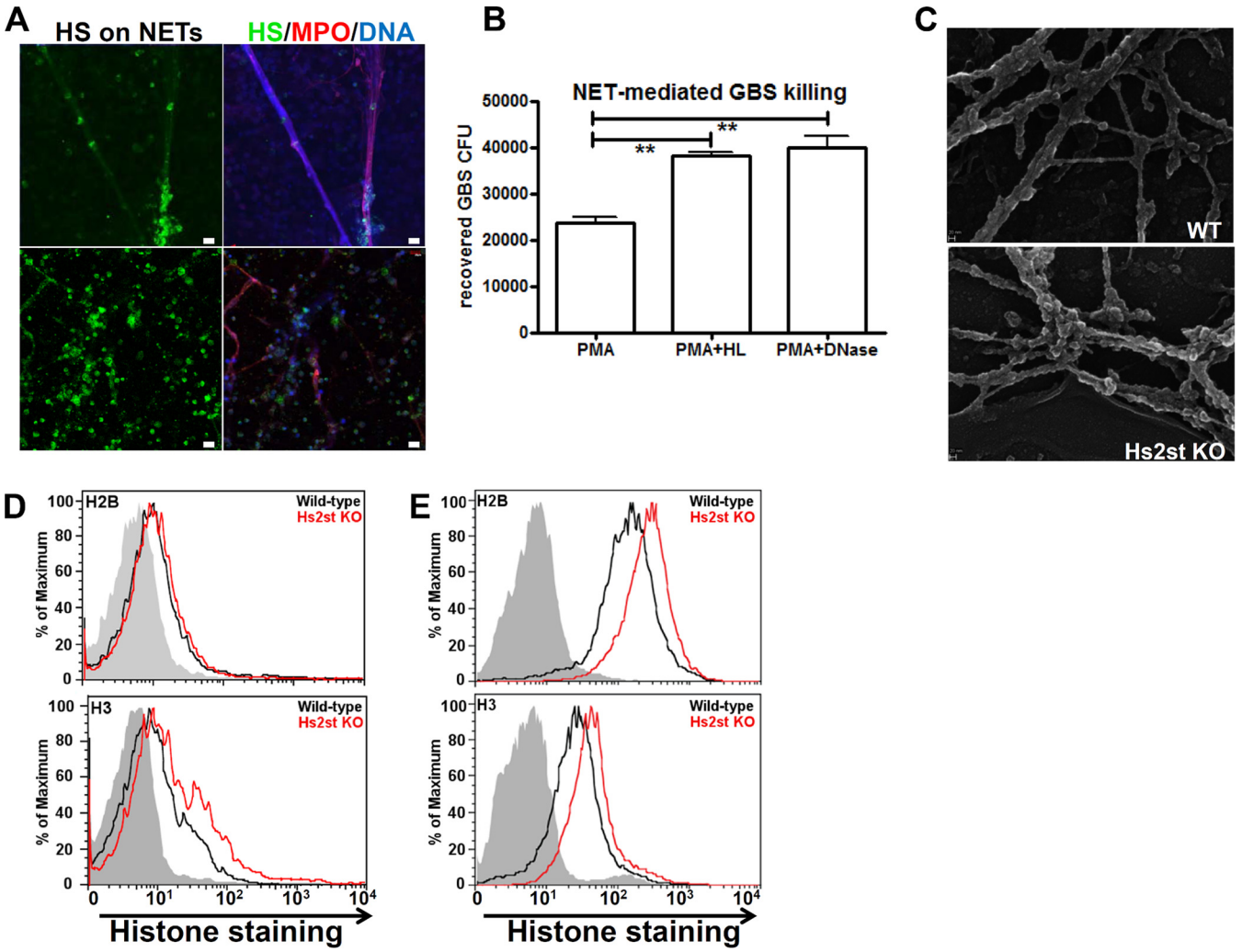

FIG 5 Reduced extracellular-trap (NET) formation in Hs2st-deficient neutrophils. (A) Human neutrophils were treated with 25 nM PMA for 3 h to allow NET formation, treated with heparan lyase III (5 mU/ml), fixed, and stained with mouse anti-stub heparan sulfate MAb, rabbit anti-myeloperoxidase PAb, and DAPI, followed by appropriate fluorochrome-conjugated secondary antibodies. (B) Human neutrophils were treated with 25 nM PMA for 3 h to induce NET formation and then treated with DNase I (10 U/ml) or heparan lyase I and III (5 mU/ml) for 30 min at 37°C, followed by incubation with GBS for 30 min. Surviving GBS were enumerated by serial plating. Differences between groups were calculated by unpaired *t* test. **, $P < 0.01$; *, $P < 0.05$. (C) Scanning electron microscopy image of NETs produced by the PMA-activated neutrophils collected from WT or Hs2st-deficient mice. (D) Binding of histone H2B and H3 (both at 5 μg/ml) to peripheral neutrophils isolated from WT and Hs2st-deficient mice. (E) Binding of histone H2B and H3 (both at 5 μg/ml) to endothelial cells isolated from WT and Hs2st-deficient mice.

pacity for histones (Fig. 5D). To better assess the effect of Hs2st deficiency on histone binding, we also examined binding to Hs2st-deficient endothelial cells, which express HS in much higher quantities than neutrophils. Indeed, histones showed strong binding to endothelial cells, and both histones H2B and H3 bound HS expressed on the surface of Hs2st-deficient endothelial cells at a level 2-fold greater than that seen with wild-type endothelial cells (Fig. 5E).

DISCUSSION

Neutrophils are typically the first immune cells to arrive in large numbers at infection sites in response to microbe-derived chemotactic signals and cytokines secreted by tissue-resident cells. Circulating neutrophils first engage the microvascular endothelium close to the inflammatory site and, after rolling on the endothelium, extravasate into the tissue (31, 32). Once in the tissues, neutrophils can be fully activated to combat and constrain infections and orchestrate other cells of the immune system. The absence of neutrophils or impairment of neutrophil recruitment and activation can allow access of invading pathogens to the systemic circulation and increase the risk of fatal sepsis. We previously found that altered sulfation on endothelial cell HS by inactivation of uronyl 2-*O*-sulfotransferase (Hs2st) promoted neutrophil adhesion and extravasation in a sterile inflammation model mediated by enhanced chemokine and L-selectin binding (11). Here, we unexpectedly found that Hs2st-deficient mice did not experience an immune benefit from the accelerated recruitment of neutrophils but instead were more susceptible to infection with live bacteria. This phenotype reflects a combination of increased endothelial cell death and barrier dysfunction and reduced NET-mediated neutrophil killing.

The structure of NETs is crucial in bacterial entrapment and

provides a high local concentration of extracellular antimicrobial factors. HS is detected in NETs, overlapping in distribution with the well-characterized microbicidal enzyme MPO (Fig. 5A). Removal of neutrophil surface HS by heparin lyase treatment reduced neutrophil NET-mediated bactericidal activities, suggesting that the origin of the HS in the NET is cell surface HSPGs (33) (Fig. 5B). Direct bacterial killing has previously been linked to highly toxic modified histones (34, 35). Recently, exogenously administered nonanticoagulant heparin (a highly sulfated form of HS) was found to colocalize with NETs, possibly through binding to the NET histones, with consequent reduction of the cytotoxicity of the heparin-bound histone (21). In accordance with the poor bactericidal activity of Hs2st-deficient neutrophils, inactivation of Hs2st was associated with increased histone binding to neutrophil surface HS (Fig. 5D and E). Therefore, in addition to the reduced NET formation, sequestering of histones on the HS may further contribute to the impaired bactericidal activity of Hs2st-deficient neutrophils.

Generally reduction of sulfation on HS decreases its binding affinity for most ligands, presumably through removal of negatively charged domains mediating key electrostatic interactions. However, the net charge of HS extracted from the Hs2st-deficient cells is similar to that from wild-type cells due to increased *N*-sulfation and 6-*O*-sulfation of the glucosamine residues, which apparently enhances the interaction of the highly positively charged histones, as observed previously for IL-8 (11). Interactions between cell surface proteoglycans and histones or neutrophil granule proteases have been demonstrated (14, 20, 36, 37); however, whether proteoglycans are a component of NETs and whether HS sulfation may modulate the quantity, location, or function of histones on NETs had not been addressed previously. Our data indicate that inactivation of Hs2st on neutrophils may impair their bactericidal activity through reduced NET formation and potentially enhance sequestration of histone from delivery to the bacterial cell wall target. Under pathological conditions in which there is significant cell activation or death, histones are released into the circulation, where they can exert cytotoxic activity on vascular endothelium (22, 38). Histone release also has been suggested to trigger a feedback cascade, resulting in more cell death and additional release of histones (39). Enhanced adherence of GBS to Hs2st-deficient endothelial cells led to more cell death upon infection (Fig. 2C and D). Should histone release be triggered in this context, the increased binding of histones (Fig. 5E) could exacerbate endothelial cell death and microvascular dysfunction upon GBS infection.

Recognized as a danger-associated molecular pattern (DAMP), extracellular histones can modulate and amplify the inflammatory response through Toll-like receptor-2 (TLR-2), TLR-4, and NLRP3 inflammasome activation (40–42). Hs2st-deficient macrophages responded normally to TLR stimuli (Fig. 3); however, Hs2st-deficeint neutrophils were significantly less capable of killing GBS *in vitro* (Fig. 4), consistent with the observed innate immune defect *in vivo*.

In summary, we have demonstrated that loss of brain endothelial cell integrity and reduced NET-mediated host defense may combine to yield the unexpected susceptibility of Hs2St-deficient mice to GBS infection. Inactivation of Hs2st in neutrophils also impacts the binding capacity of histones, a critical antimicrobial molecule and structure on the NETs, revealing an unexplored role for HS in neutrophil NET biology.

ACKNOWLEDGMENTS

This work was supported by the NHLBI-sponsored UCSD Program in Excellence in Glycosciences (HL107150 to V.N. and J.D.E.), grant 13BGIA14150008 from the American Heart Association (to D.X.), and additional NIH/NIAID and NIH/NHLBI grants to J.D.E. and V.N.

We thank the UCSD Histology Core, also supported though HL107150, for technological and instrumental support. We thank Ying Jones, Timo Meerloo, and Marilyn G. Farquhar of the UCSD Electron Microscopy Facility and Jennifer Santini of the UCSD Neuroscience Microscopy Shared Facility for advice and assistance with instrumentation. The UCSD Neuroscience Microscopy Shared Facility is supported by a Center Core Grant from the National Institute of Neurological Disorders and Stroke (P30 NS047101).

REFERENCES

1. **Bishop JR, Schuksz M, Esko JD.** 2007. Heparan sulphate proteoglycans fine-tune mammalian physiology. Nature **446:**1030–1037. http://dx.doi.org/10.1038/nature05817.
2. **Sarrazin S, Lamanna WC, Esko JD.** 2011. Heparan sulfate proteoglycans. Cold Spring Harbor Perspect Biol **3:**1–33. http://dx.doi.org/10.1101/cshperspect.a004952.
3. **Xu D, Esko JD.** 2014. Demystifying heparan sulfate-protein interactions. Annu Rev Biochem **83:**129–157. http://dx.doi.org/10.1146/annurev-biochem-060713-035314.
4. **Lindahl U, Kjellen L.** 2013. Pathophysiology of heparan sulphate: many diseases, few drugs. J Intern Med **273:**555–571. http://dx.doi.org/10.1111/joim.12061.
5. **Rostand KS, Esko JD.** 1997. Microbial adherence to and invasion through proteoglycans. Infect Immun **65:**1–8.
6. **Teng YH, Aquino RS, Park PW.** 2012. Molecular functions of syndecan-1 in disease. Matrix Biol **31:**3–16. http://dx.doi.org/10.1016/j.matbio.2011.10.001.
7. **Tiwari V, Maus E, Sigar IM, Ramsey KH, Shukla D.** 2012. Role of heparan sulfate in sexually transmitted infections. Glycobiology **22:**1402–1412. http://dx.doi.org/10.1093/glycob/cws106.
8. **Parish CR.** 2006. The role of heparan sulphate in inflammation. Nat Rev Immunol **6:**633–643. http://dx.doi.org/10.1038/nri1918.
9. **Mayadas TN, Cullere X, Lowell CA.** 2014. The multifaceted functions of neutrophils. Annu Rev Pathology **9:**181–218. http://dx.doi.org/10.1146/annurev-pathol-020712-164023.
10. **Nathan C.** 2006. Neutrophils and immunity: challenges and opportunities. Nat Rev Immunol **6:**173–182. http://dx.doi.org/10.1038/nri1785.
11. **Axelsson J, Xu D, Kang BN, Nussbacher JK, Handel TM, Ley K, Sriramarao P, Esko JD.** 2012. Inactivation of heparan sulfate 2-O-sulfotransferase accentuates neutrophil infiltration during acute inflammation in mice. Blood **120:**1742–1751. http://dx.doi.org/10.1182/blood-2012-03-417139.
12. **Wang L, Fuster M, Sriramarao P, Esko JD.** 2005. Endothelial heparan sulfate deficiency impairs L-selectin- and chemokine-mediated neutrophil trafficking during inflammatory responses. Nat Immunol **6:**902–910.
13. **Garner OB, Yamaguchi Y, Esko JD, Videm V.** 2008. Small changes in lymphocyte development and activation in mice through tissue-specific alteration of heparan sulphate. Immunology **125:**420–429. http://dx.doi.org/10.1111/j.1365-2567.2008.02856.x.
14. **Campbell EJ, Owen CA.** 2007. The sulfate groups of chondroitin sulfate- and heparan sulfate-containing proteoglycans in neutrophil plasma membranes are novel binding sites for human leukocyte elastase and cathepsin G. J Biol Chem **282:**14645–14654. http://dx.doi.org/10.1074/jbc.M608346200.
15. **Glenthoj A, Cowland JB, Heegaard NH, Larsen MT, Borregaard N.** 2011. Serglycin participates in retention of alpha-defensin in granules during myelopoiesis. Blood **118:**4440–4448. http://dx.doi.org/10.1182/blood-2011-06-362947.
16. **Niemann CU, Abrink M, Pejler G, Fischer RL, Christensen EI, Knight SD, Borregaard N.** 2007. Neutrophil elastase depends on serglycin proteoglycan for localization in granules. Blood **109:**4478–4486. http://dx.doi.org/10.1182/blood-2006-02-001719.
17. **Brinkmann V, Reichard U, Goosmann C, Fauler B, Uhlemann Y, Weiss DS, Weinrauch Y, Zychlinsky A.** 2004. Neutrophil extracellular traps kill bacteria. Science **303:**1532–1535. http://dx.doi.org/10.1126/science.1092385.

18. **Papayannopoulos V, Zychlinsky A.** 2009. NETs: a new strategy for using old weapons. Trends Immunol **30:**513–521. http://dx.doi.org/10.1016/j.it.2009.07.011.
19. **Freeman CG, Parish CR, Knox KJ, Blackmore JL, Lobov SA, King DW, Senden TJ, Stephens RW.** 2013. The accumulation of circulating histones on heparan sulphate in the capillary glycocalyx of the lungs. Biomaterials **34:**5670–5676. http://dx.doi.org/10.1016/j.biomaterials.2013.03.091.
20. **Watson K, Gooderham NJ, Davies DS, Edwards RJ.** 1999. Nucleosomes bind to cell surface proteoglycans. J Biol Chem **274:**21707–21713. http://dx.doi.org/10.1074/jbc.274.31.21707.
21. **Wildhagen KC, Garcia de Frutos P, Reutelingsperger CP, Schrijver R, Areste C, Ortega-Gomez A, Deckers NM, Hemker HC, Soehnlein O, Nicolaes GA.** 2014. Nonanticoagulant heparin prevents histone-mediated cytotoxicity in vitro and improves survival in sepsis. Blood **123:**1098–1101. http://dx.doi.org/10.1182/blood-2013-07-514984.
22. **Xu J, Zhang X, Pelayo R, Monestier M, Ammollo CT, Semeraro F, Taylor FB, Esmon NL, Lupu F, Esmon CT.** 2009. Extracellular histones are major mediators of death in sepsis. Nat Med **15:**1318–1321. http://dx.doi.org/10.1038/nm.2053.
23. **Perriere N, Demeuse P, Garcia E, Regina A, Debray M, Andreux JP, Couvreur P, Scherrmann JM, Temsamani J, Couraud PO, Deli MA, Roux F.** 2005. Puromycin-based purification of rat brain capillary endothelial cell cultures. Effect on the expression of blood-brain barrier-specific properties. J Neurochem **93:**279–289.
24. **Chang YC, Wang Z, Flax LA, Xu D, Esko JD, Nizet V, Baron MJ.** 2011. Glycosaminoglycan binding facilitates entry of a bacterial pathogen into central nervous systems. PLoS Pathog **7:**e1002082. http://dx.doi.org/10.1371/journal.ppat.1002082.
25. **Da Costa AF, Pereira CS, Santos Gda S, Carvalho TM, Hirata R, Jr, De Mattos-Guaraldi AL, Rosa AC, Nagao PE.** 2011. Group B Streptococcus serotypes III and V induce apoptosis and necrosis of human epithelial A549 cells. Int J Mol Med **27:**739–744. http://dx.doi.org/10.3892/ijmm.2011.635.
26. **Kling DE, Tsvang I, Murphy MP, Newburg DS.** 2013. Group B Streptococcus induces a caspase-dependent apoptosis in fetal rat lung interstitium. Microb Pathog **61-62:**1–10. http://dx.doi.org/10.1016/j.micpath.2013.04.008.
27. **Reiss A, Braun JS, Jager K, Freyer D, Laube G, Buhrer C, Felderhoff-Muser U, Stadelmann C, Nizet V, Weber JR.** 2011. Bacterial pore-forming cytolysins induce neuronal damage in a rat model of neonatal meningitis. J Infect Dis **203:**393–400. http://dx.doi.org/10.1093/infdis/jiq047.
28. **Ulett GC, Bohnsack JF, Armstrong J, Adderson EE.** 2003. Beta-hemolysin-independent induction of apoptosis of macrophages infected with serotype III group B streptococcus. J Infect Dis **188:**1049–1053. http://dx.doi.org/10.1086/378202.
29. **Doran KS, Chang JC, Benoit VM, Eckmann L, Nizet V.** 2002. Group B streptococcal beta-hemolysin/cytolysin promotes invasion of human lung epithelial cells and the release of interleukin-8. J Infect Dis **185:**196–203. http://dx.doi.org/10.1086/338475.
30. **Ermert D, Urban CF, Laube B, Goosmann C, Zychlinsky A, Brinkmann V.** 2009. Mouse neutrophil extracellular traps in microbial infections. J Innate Immun **1:**181–193. http://dx.doi.org/10.1159/000205281.
31. **Borregaard N.** 2010. Neutrophils, from marrow to microbes. Immunity **33:**657–670. http://dx.doi.org/10.1016/j.immuni.2010.11.011.
32. **Kolaczkowska E, Kubes P.** 2013. Neutrophil recruitment and function in health and inflammation. Nat Rev Immunol **13:**159–175. http://dx.doi.org/10.1038/nri3399.
33. **Petersen F, Brandt E, Lindahl U, Spillmann D.** 1999. Characterization of a neutrophil cell surface glycosaminoglycan that mediates binding of platelet factor 4. J Biol Chem **274:**12376–12382. http://dx.doi.org/10.1074/jbc.274.18.12376.
34. **Hirsch JG.** 1958. Bactericidal action of histone. J Exp Med **108:**925–944. http://dx.doi.org/10.1084/jem.108.6.925.
35. **Parseghian MH, Luhrs KA.** 2006. Beyond the walls of the nucleus: the role of histones in cellular signaling and innate immunity. Biochem Cell Biol **84:**589–604. http://dx.doi.org/10.1139/o06-082.
36. **Kubota T, Kanai Y, Miyasaka N.** 1990. Interpretation of the cross-reactivity of anti-DNA antibodies with cell surface proteins: the role of cell surface histones. Immunol Lett **23:**187–193. http://dx.doi.org/10.1016/0165-2478(90)90190-2.
37. **Ojcius DM, Muller S, Hasselkus-Light CS, Young JD, Jiang S.** 1991. Plasma membrane-associated proteins with the ability to partially inhibit perforin-mediated lysis. Immunol Lett **28:**101–108. http://dx.doi.org/10.1016/0165-2478(91)90106-K.
38. **Saffarzadeh M, Juenemann C, Queisser MA, Lochnit G, Barreto G, Galuska SP, Lohmeyer J, Preissner KT.** 2012. Neutrophil extracellular traps directly induce epithelial and endothelial cell death: a predominant role of histones. PLoS One **7:**e32366. http://dx.doi.org/10.1371/journal.pone.0032366.
39. **Chaput C, Zychlinsky A.** 2009. Sepsis: the dark side of histones. Nat Med **15:**1245–1246. http://dx.doi.org/10.1038/nm1109-1245.
40. **Allam R, Darisipudi MN, Tschopp J, Anders HJ.** 2013. Histones trigger sterile inflammation by activating the NLRP3 inflammasome. Eur J Immunol **43:**3336–3342. http://dx.doi.org/10.1002/eji.201243224.
41. **Allam R, Scherbaum CR, Darisipudi MN, Mulay SR, Hagele H, Lichtnekert J, Hagemann JH, Rupanagudi KV, Ryu M, Schwarzenberger C, Hohenstein B, Hugo C, Uhl B, Reichel CA, Krombach F, Monestier M, Liapis H, Moreth K, Schaefer L, Anders HJ.** 2012. Histones from dying renal cells aggravate kidney injury via TLR2 and TLR4. J Am Soc Nephrol **23:**1375–1388. http://dx.doi.org/10.1681/ASN.2011111077.
42. **Xu J, Zhang X, Monestier M, Esmon NL, Esmon CT.** 2011. Extracellular histones are mediators of death through TLR2 and TLR4 in mouse fatal liver injury. J Immunol **187:**2626–2631. http://dx.doi.org/10.4049/jimmunol.1003930.